ELSEVIER

Ceramics International 25 (1999) 257–260

CERAMICS INTERNATIONAL

# Modeling of fiber toughening in fiber-reinforced ceramic composites

G.M. Song*, Y. Zhou, Y. Sun

*School of Materials Science and Engineering, PO Box 433 Harbin Institute of Technology, Harbin 150001, P. R. China*

Received 26 August 1997; accepted 5 February 1998

**Abstract**

A fiber toughening model of fiber-reinforced ceramic matrix composites is presented. The constitutive equation is obtained through micromechanical considerations based on two kinds of fiber toughening mechanisms, crack bridging and fiber pullout. The calculated results show that two different zones in the *R*-curve and Load/displacement curve exhibit notable nonlinear behavior. Calculated toughness of 50 vol%$SiC_f$/LAS composites is in good agreement with experimental results. 

## 1. Introduction

Fracture toughness of ceramic materials can be improved remarkably by incorporating fibers [1–4]. When a macroscopic crack propagates in ceramic matrix, some fibers with higher strength will bridge the crack, and some fibers with lower strength will break either within the crack faces or within the matrix. It shows that intact fiber bridging and broken fiber pullout operate simultaneously. The fracture resistance is provided by the development of fiber bridging and fiber pullout in the crack wake, so the intervening fracture resistance curve, or *R* curve in fiber-reinforced ceramics is of great interest. Several theoretical analyses of the fiber bridging process have been proposed [5–7], and a model of fiber pullout based on weakest-link statistics is also provided by Thouless and Evans [4]. Nevertheless all these works are for a static crack. In this study, a model including both fiber bridging and fiber pullout was provided and used to calculate *R*-curve of a propagating crack.

## 2. Theoretical model

When a crack propagates perpendicularly to the fibers in unidirectional fiber-reinforced ceramics with a weak fiber/matrix interface, fibers debond from the matrix and slip over a certain distance, $l_s$ (Fig. 1). The relation between the fiber stress, $\sigma_b$, and the crack opening displacement, $u$, can be obtained according to the shear-lag model [8]

$$\sigma_b = [E_f\tau(1+\eta)/r]^{1/2}\sqrt{u} \tag{1}$$

where $E_f$ and $r$ are the Young's modulus and the radius of the fiber, $\tau$ is the fiber/matrix shear stress, and $\eta = E_fV_f/(E_mV_m)$ and with $E_m$ being the matrix modulus, and $V_m = 1 - V_f$ the volume fraction of the matrix.

As the crack extends and opens, the intact fibers will eventually fail. For these broken fibers, the pullout stress, $\sigma_p$, at the crack plane is

$$\begin{aligned} \sigma_p &= \frac{2\tau}{r}(\langle h\rangle - u) && (\langle h\rangle > u) \\ \sigma_p &= 0 && (\langle h\rangle < u) \end{aligned} \tag{2}$$

where $\langle h\rangle$ denotes the mean pullout length of the fibers.

Fiber strength distribution is presumed to satisfy the weakest-link statistics, and the explicit form is given by the two-parameter Weibull distribution, $S$ and $m$, $S$ is the scale parameter and $m$ is the shape parameter. Then the mean strength [4], $\langle\sigma\rangle$, of all fibers is

$$\langle\sigma\rangle = s\Gamma[(2+m)/(1+m)] \tag{3}$$

If there are enough fibers in the crack wake zone to apply the statistical analysis, the expression for the average stress, $\sigma$, at an opening, $u$, is thus

* Corresponding author.

0272-8842/99/$—see front matter 
PII: S0272-8842(98)00033-9

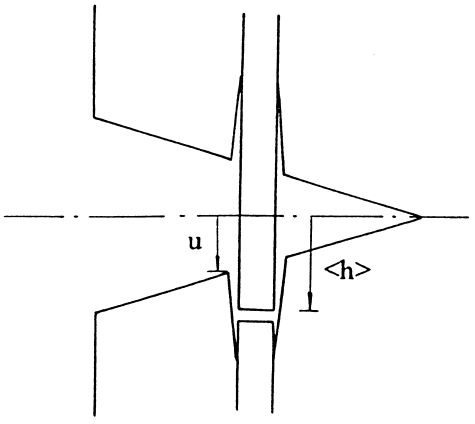


Fig. 1. Schematic of fiber bridging matrix crack.

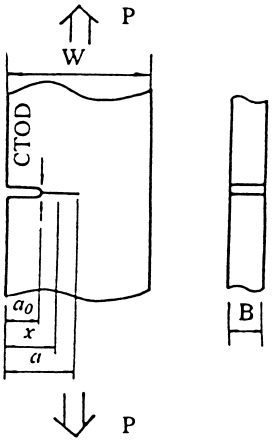


Fig. 2. Single edged notch tension specimen.

$$\frac{\sigma(u)}{V_f} = e^{-\phi(u)}\sigma_b + (1 - e^{-\phi(u)})\sigma_p \qquad (u < u_c)$$
$$\frac{\sigma(u)}{V_f} = 0 \qquad (u > u_c) \tag{4}$$

where $\phi(u) = \left[\frac{4\tau E_f(1+\eta)u}{S^2 r}\right]^{m+1}$, $e^{-\Phi(u)}$ is the fraction of non-broken fiber at opening displacement, $u$, and $\sigma_p$ is the average value of the pullout stress [Eq. (2)] based on the average failure length, $\langle h\rangle$, associated with all prior failure, which is

$$\langle h\rangle = \frac{r}{2\tau}\frac{S\int_0^{\phi(u)}\beta^{1/(m+1)}e^{-\beta}d\beta}{2\tau(m+1)(\eta+1)}$$

Fig. 2 shows a single notch tension specimen, the stress intensity factor, $K_p$ due to an external load, $P$, is given as

$$K_p(a) = \frac{P\sqrt{a\pi}}{BW}F(a/W) \tag{5}$$

where $a$ is the crack length, $B$ is specimen thickness and $W$ is the width, as shown in Fig. 2. $F(a/W)$ is a weight function [9].

Similarly, stress intensity $\Delta K_b$ for the unbroken fibers is

$$\Delta K_p = \int_{a_o}^{a}\frac{2V_f e^{-\phi(u)}\sigma_b(u(x))}{\sqrt{\pi a}}H(a/W, x/a)\mathrm{d}x \tag{6}$$

and stress intensity factor, due to the pullout stress of the failed fibers is

$$\Delta K_p = \int_{a_o}^{a}\frac{2V_f(1 - e^{-\phi(u)})\sigma_p(u(x))}{\sqrt{\pi a}}H(a/W, x/a)\mathrm{d}x \tag{7}$$

where $x$ is as shown in Fig. 2, and $H(a/W, x/a)$ is a corresponding weight function [9].

For the notched specimen geometry, the initial notch length, $a_0$, is much longer than the growing crack length, $\Delta a(= a - a_0)$, as long as the crack propagation is unstable. We assume that the crack faces remain straight during crack propagation, thus the opening displacement at point $x$ is

$$2u(a, x) = \alpha(a - x) \qquad (a_0 \le x \le a) \tag{8}$$

with $a$ being the angle between the crack faces. Then the crack tip opening displacement, CTOD, is obtained by

$$\mathrm{CTOD} = 2u(a, a_0) = C_p(a, a_0)$$
$$P - \int_{a_0}^{a} C_x(a, a_0, x)\sigma[u(a, x)]\mathrm{d}x \tag{9}$$

where

$$C_p(a, a_0) = \frac{2}{E}\int_{a_0}^{a}\left[\frac{\sqrt{a\pi}}{BW}F(a/W)\right]\left[\frac{2}{\sqrt{\pi a}}H(a/W, a_0/a)\right]\mathrm{d}a$$

$$C_x(a, a_0, x) = \frac{2}{E}\int_{x}^{a}\left[\frac{2}{\sqrt{\pi a}}H(a/W, x/a)\right]\left[\frac{2}{E}H(a/W, a_0/a)\right]\mathrm{d}a$$

As a crack propagates, the fracture resistance, $K_r$, of the material is given by

$$K_r(a) = K_m + \Delta K_b(a) + \Delta K_p(a) \tag{10}$$

where $K_m$ is the matrix toughness, $K_b$ and $K_p$ represent the effects of fiber bridging and fiber pullout, respectively. The condition for crack propagation is

$$K_p(a) \ge K_r(a) \tag{11}$$

Eq. (10) combines the fiber bridging and fiber pullout effects. The complete fracture resistance curve, or *R*-curve, and load/displacement curve can be obtained using Eqs. (10) and (11), The fracture toughness, $K_{IC}$, and the contributions, $K_b$ and $K_p$, are given at the point of maximum load, $P_{max}$, where crack propagating instability will occur under increasing load control condition.

## 3. Results and discussion

A typical lithium-alumino-silicate ceramic matrix reinforced with Nicalon silicon carbide fibers ($SiC_f$/LAS) is used to carried out the quantitative analysis of fiber toughening effect. Its microstructure and mechanical properties have been studied in detail [1,2,10]. Fiber properties are $E_f = 200$ GPa, $r = 0.6$ mm, and $V_f = 0.5$. The Young's modulus of the matrix is $E_m = 85$ GPa, and the fracture toughness is $K_m = 2\,\mathrm{MPam}^{1/2}$. The tensile strength of this composite is about 600 MPa [2], which implies that the mean strength of the fibers in this composite is 1200 GPa or so, much lower than the as-fabricated strength (2060 MPa) of the fiber. So $\langle\sigma_f\rangle$ is taken as 1200 MPa. The fiber flaw distribution parameter is $m = 3.2$. The measured value of fiber/matrix interface shear stress, $\tau$, is 3.5–3.6 MPa in the first time push measurement [3], which is higher than the values (2.0 MPa) of subsequent measurements. We take $\tau$ as 3.5 MPa.

For a tensile specimen (Fig. 2), the initial crack length is $a_0 = 20$ mm, the width, $W = 40$ mm, and the thickness, $B = 10$ mm. The load, $P$, associated with an applied stress intensity, $K_p$, is given by Eq. (5), the crack resistance, $K_r$, can also be obtained by Eq. (10). If $K_p < K_r$, $P$ increases, the stress calculations are repeated. If $K_p = K_r$ , the main crack, $a$, extend a small increment, d$a$, and then all the stress calculation are repeated again. The whole calculation process is redone until the main crack propagates in an unstable manner.

The crack growth curve exhibits two stages characterized by a significant change in slope (Fig. 3). Initially, the fracture resistance increases rapidly with crack propagating due to intact fibers behind the crack tip. The relation between stress, $\sigma$, and displacement, $u$, for a crack surface bridged by fiber is depicted in Fig. 4, where the fiber bridging is the dominant mechanism immediately behind the crack tip, and the crack opening displacements are of the order of a few microns. The end of first stage is attained when the cohesive stress at the notch tip reaches its peak value. In the second stage, many intact fibers will break with further crack propagation, which lowers bridging toughening but enhances fiber pullout toughening. The overall toughening contribution during the second stage is usually small compared with the fracture resistance at the instability point. It implies that the bridging is the dominant toughening mechanism in fiber-reinforced ceramics.

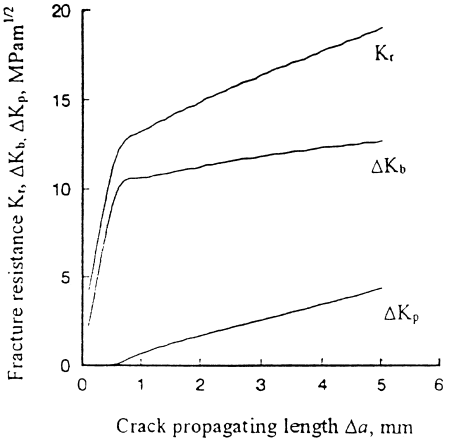


Fig. 3. Fracture resistance curve versus crack propagating length.

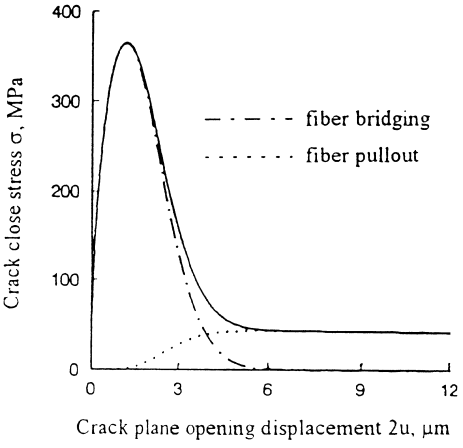


Fig. 4. Crack close stress versus crack plane opening displacement.

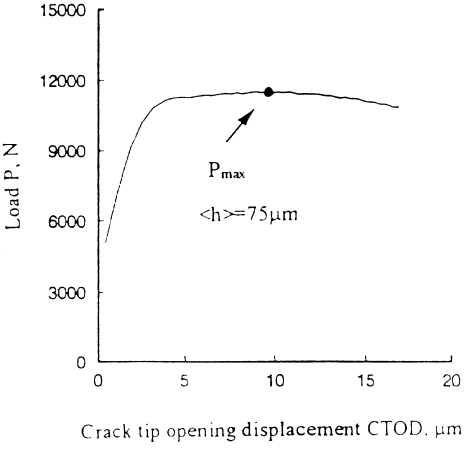


Fig. 5. Load/displacement curve.

However, most of the stable crack growth take place in the second stage. The corresponding load/displacement curve is shown in Fig. 5. At the peak load, $P_{max}$, the crack tip opening displacement, CTOD, is 9.8 μm, lower than the average fiber pull length, $\langle h\rangle$ (= 75μm). Because more fibers fail which lowers the fiber bridging

contribution when the crack propagates continuously, the load $P$ will be gradually decreased after the peak load, $P_{max}$.

In the first zone of the $R$-curve, the external load, $P$, increases fast with crack tip opening. While in the second zone, $P$ increases slowly until reaching the peak point, $P_{max}$, where the fracture toughness, $K_{IC}$, and the contributions from fiber bridging toughening and fiber pullout toughening, $\Delta K_b$, $\Delta K_p$, are 15.71 $MPam^{1/2}$, 11.5 $MPam^{1/2}$ and 2.21 $MPam^{1/2}$, respectively. In this study, the toughening due to fiber bridging is more significant than that of fiber pullout, and the calculated fracture toughness, 15.71 $MPam^{1/2}$, is close to the experimental result [1], 17 $MPam^{1/2}$.

## References

[1] J.J. Brennan, K.M. Prewo, Silicon carbide fiber reinforced glass-ceramic matrix composites exhibiting high strength and toughness, J. Mater. Sci. 17 (1982) 2371–2383.

[2] D.B. Marshall, A.G. Evans, Failure mechanisms in ceramic-fiber/ceramic-matrix composites, J. Am. Ceram. Soc. 68 (1985) 225–231.

[3] D.B. Marshall, W.C. Oliver, Measurement of interfacial mechanical properties in fiber-reinforced ceramic composites, J. Am. Ceram. Soc. 70 (1987) 542–548.

[4] M.D. Thouless, A.G. Evans, Effects of pull-out on mechanical properties of ceramic-matrix composites, Acta Metall. 36 (1988) 517–522.

[5] B. Budiansky, J.W. Hutchinson, A.G. Evans, Matrix fracture in fiber reinforced ceramics, J. Mech. Phys. Solids 34 (1986) 167–189.

[6] L.N. McCartney, Mechanics of matrix cracking in brittle-matrix fiber reinforced composites, Pro. R. Soc. London A409 (1987) 329–350.

[7] Y.C. Chiang, A.S.D. Wang, T.W. Chou, On matrix cracking in fiber reinforced ceramics, J. Mech. Phys. Solids 42 (1993) 1137–1154.

[8] D.B Marshall, B.N. Cox, A.G. Evans, The mechanics of matrix cracking in brittle-matrix fiber composites, Acta Metall. 33 (1985) 2013–2021.

[9] H., Tada, P.C., Paris, G.R., Irwin, The Stress Analysis of Cracks Handbook, Del Research Corporation, Hellertown, PA, 1973, pp.2,16–27.

[10] G. Simon, A.R. Bunsell, Mechanical and structural characterization of the Nicalon silicon carbon fiber, J. Mater. Sci. 19 (1984) 3649–3657.